Applied Mathematics and Mechanics
(English Edition, Vol 23, No 6, Jun 2002)
Published by Shanghai University, Shanghai, China

Article ID: 0253-4827(2002)06-0694-09

THEORETICAL ANALYSIS OF USING AIRFLOW TO PURGE RESIDUAL WATER IN AN INCLINED PIPE *

SHEN Fang (沈 芳)[1], YAN Zong-yi (严宗毅)[1],
ZHAO Yao-hua (赵耀华)[2], Kiyoshi Horii[3]

(1. Department of Mechanics and Engineering Science, Peking University, Beijing 100871, P R China;
2. Institute of Engineering Thermophysics, Chinese Academy of Sciences, Beijing 100080, P R China;
3. Shirayuri College, Tokyo, Japan)

(Communicated by WU Wang-yi)

Abstract: A refined theoretical analysis for using the spiral airflow and axial airflow to purge residual water in an inclined pipe was presented. The computations reveal that, in most cases, the spiral flow can purge the residual water in the inclined pipe indeed while the axial flow may induce back flow of the water, just as predicted in the experiments presented by Horii and Zhao et al. In addition, the effects of various initial conditions on water purging were studied in detail for both the spiral and axial flow cases.

Key words: spiral flow; axial flow; water purging; two-phase flow; pipe flow
CLC number: O35+.1 Document code: A

Introduction

Purging residual liquid in a U-shaped pipeline is challenge for chemical and transportation industry[1]. Many techniques have been employed to purge out residual water[2], but none have been completely satisfactory. One possible method for doing this has been to blow a great quantity of compressed air through the pipeline. When a short line is plugged with water columns, it is possible to purge out the residual water. However, when the length of pipeline is long and U-shaped sections are included, it is inadequate to remove it completely.

In the early 1990s, Horii put forward the conception of spiral flow[3, 4]. Different from the axial flow (airflow in a pipeline which is parallel to the axis), the airflow in spiral flow moves not only along the axis, but also around the circumference of the pipeline. So when spiral airflow was employed, the surface of residual water was sheared off and blown toward the inclined section of the pipe to form a water film, and was purged out completely in spiral way. Recently,

* Received date: 2000-11-15; Revised date: 2001-11-28
Foundation item: the National High Capability Calculation Foundation of China (981006)
Biography: SHEN Fang (1977 -), Doctor (E-mail: shenfang@sina.com)

Horii, Zhao, Tomita and Shimo have made experiments to show that the spiral airflow could remove the residual water completely in an inclined pipeline[5]. Fig. 1 shows their experiment model. The pipeline consisted of 79mm-diameter pipes over a distance of 129m including the U-shaped pipe section of 2.6m. Experiments were performed to test removal of 0.07m^3-water. The pressure of both device tubes arose to 200 kPa-gage and developed an average pipe flow velocity of 20m/s. In order to make comparison, airflow was generated by either the spiral flow device or the axial flow device and experiments were conducted varying the inclination angle of the pipe. Their experimental results showed that the spiral flow could efficiently purge the residual water out of the inclined pipe while in the axial turbulent flow the water often flows back after it was driven forward for a distance.

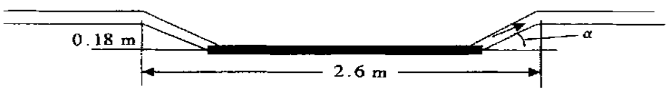

Fig. 1 The experimental apparatus of Ref. [5]

Referring to the experimental result of Ref. [5], we present a simplified theoretical model herein. The principle of mass and momentum conservation is applied to the thin water layer from Lagrangian viewpoint and, thus, governing equations similar to the momentum integral equation in the boundary layer theory are derived. Variable thickness of the layer and a third order polynomial approximation for the velocity profile are considered.

1 The Varying Thickness Model for Axial Flow

1.1 Simplification of geometry

Fig. 2 shows a circular pipe of radius r_0, which is inclined at angle α with respect to the horizontal direction. The residual water inside it corresponds to angle θ with respect to the center of the circle. We usual consider the thickness of the residual water to be far smaller than the radius of pipeline, and we may treat it as a problem of water flowing up over an inclined plane of width $r_0\theta$. The equivalent thickness of the water layer h_0 can be derived. From the equality of the cross-section areas of the water in the two geometries, we have $r_0\theta h_0 = r_0^2(\theta - \sin\theta)/2$, and thus

$$h_0 = \frac{r_0}{2}\left(1 - \frac{\sin\theta}{\theta}\right). \qquad (1)$$

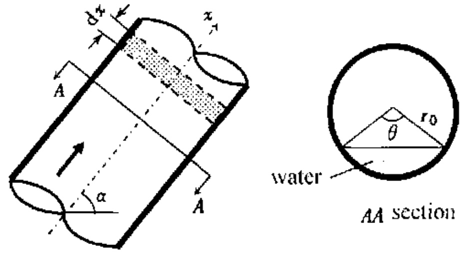

Fig. 2 Geometry of water purging out of an inclined pipe

For a small segment of air with cross-section area πr_0^2 and thickness dx in the circular pipe, the moment conservation in the x direction requires

$$-\frac{\mathrm{d}p}{\mathrm{d}x}\mathrm{d}x\pi r_0^2 = \tau_i r_0\theta\mathrm{d}x + \tau_g(2\pi - \theta) r_0\mathrm{d}x, \qquad (2)$$

where p is the pressure, τ_g is air's shear stress on the pipe wall and τ_i is air's shear stress on its interface with water. The gravity force is neglected here for air. Then the pressure gradient is given by

$$\frac{dp}{dx} = -\tau_i \frac{\theta}{\pi r_0} - \frac{\tau_g}{r_0}\left(2 - \frac{\theta}{\pi}\right). \quad (3)$$

1.2 Calculation of the shear stress on the interface

Ref. [6] gave empirical formulae for the stress on the interface on experiments. τ_g is given by

$$\tau_g = \frac{1}{2}\lambda_g \rho_g U_g^2, \ \lambda_g = 0.485 \ Re_g^{-0.28}, \ Re_g = \rho_g U_g (2 r_0)/\mu_g, \quad (4)$$

where ρ_g, μ_g, U_g are the density, dynamic viscosity, and mean velocity of air, respectively.

Air's shear stress τ_i on the interface with water is computed by

$$\tau_i = \frac{1}{2}\lambda_i \rho_g U_g^2, \quad (5)$$

where the friction coefficient λ_i is dependent on the flow pattern. The flow is Ripply when the water velocity U_i on the interface is greater than the wave speed C_λ, otherwise the flow is Pebbly.

$$\lambda_i = \begin{cases} \lambda_g [1 + 6.1 \times 10^{-5} (X^{0.8} Re_l)^{0.6} Re_g^{0.7}] & \text{for Ripple flow } (U_i > C_\lambda), \\ \lambda_g [1 + 4 X^{1.2}] & \text{for Pebble flow } (U_i < C_\lambda), \end{cases} \quad (6)$$

where $Re_l = \rho w/\mu$, ρ and μ are the density and dynamic viscosity of water, w is the volumetric flow rate of water per unit width. X is called Martinelli parameter[6], defined by

$$X^2 = \frac{\lambda_l \rho \overline{U}_l^2}{\lambda_g \rho_g U_g^2}, \quad (7)$$

where $\overline{U}_l = w/h$ is the mean velocity of water in the thin layer, λ_l is the friction coefficient of water flowing over the plane, given by

$$\lambda_l = \begin{cases} 96 Re_l^{-1} & \text{for laminar flow } (Re_l < 300), \\ 0.485 \ Re_l^{-0.28} & \text{for turbulentr flow } (Re_l > 300). \end{cases} \quad (8)$$

The wave speed C_λ is given by

$$C_\lambda = \frac{1}{2} U_i + \sqrt{U_i^2/12 + g h + \sigma k^2 h/\rho},$$

where $g = 9.81 \text{ m/s}^2$ is the gravity acceleration, $\sigma = 0.073$ N/m is the surface tension coefficient of the air-water interface, $k = 2\pi/\lambda$ is the wave number ($\lambda = 0.09$m is the wave length[5]).

Substituting Eqs. (6), (7) and (8) into Eq. (5) gives

$$\tau_i = \begin{cases} \tau_g + c_1 h^{-1.2} w^{0.6} & \text{for Pebble flow } (U_i < C_\lambda), \\ \tau_g + c_2 h^{-0.52} w^{0.91} & \text{for Ripple flow } (U_i > C_\lambda), \end{cases} \quad (9)$$

where c_1 and c_2 are constants independent of h, U_i, τ_i[7].

1.3 Mass and momentum conservation

Consider a water element of thickness h and small length l from Lagrangian viewpoint (Fig. 3). The volumetric flow rate of water per unit width is defined as $w = \int_0^h u \, dy$, mass conservation of water requires that

$$\frac{dw}{dt} = \frac{dh}{dt} U_i + \int_0^h \frac{du}{dt} dy = 0. \quad (10)$$

The momentum conservation for the water element requires

$$\rho \frac{\mathrm{d}}{\mathrm{d}t}\left(\int_0^h u l \,\mathrm{d}y\right) = (\tau_i - \tau_w)\, l - \rho g h l \sin\alpha - h\frac{\mathrm{d}p}{\mathrm{d}x} l, \tag{11}$$

where τ_w is water's shear stress on the wall. It should be noted that both length l and thickness h of the water element change with the axial position x during its movement (for a water particle, its traveled distance x is dependent on the time t, of course). It is evident that $\mathrm{d}l/\mathrm{d}t = l\partial u/\partial x$, under the assumption of steady state that the quantities at a certain axial position x are independent of t. After some laborious reduction including substitution of Eq. (3), we have

$$\frac{\mathrm{d}h}{\mathrm{d}t}U_i = -\frac{\tau_i}{\rho}\left(1+\frac{\theta h}{\pi r_0}\right) + \frac{\tau_w}{\rho} - \frac{\tau_g}{\rho}\frac{h}{r_0}\left(2-\frac{\theta}{\pi}\right) + g h \sin\alpha. \tag{12}$$

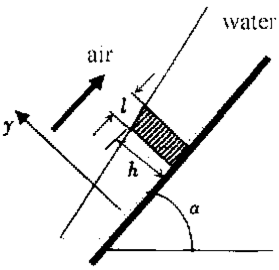

Fig. 3 The water element

1.4 The nonlinear velocity profile

We assume that the velocity profile may be represented by a third order polynomial, and it is expressed as

$$\frac{u}{U_i} = a_0 + a_1\eta + a_2\eta^2 + a_3\eta^3 \qquad \left(\eta = \frac{y}{h}\right).$$

The coefficients a_0, a_1, a_2 and a_3 can be solved by applying the boundary conditions below (They are not listed here for the sake of saving space. The details of them are listed in Ref. [7]).

$$\eta = 1: u = U_i,\ \mu\frac{\partial u}{\partial y} = \tau_i,$$

$$\eta = 0: u = 0,$$

$$\mu\frac{\partial^2 u}{\partial y^2} = \frac{\mathrm{d}p}{\mathrm{d}x} + \rho g \sin\alpha^{[8,9]} = -\tau_i\frac{\theta}{\pi r_0} - \tau_g\left(2-\frac{\theta}{\pi}\right)\frac{1}{r_0} + \rho g \sin\alpha,$$

so

$$u = U_i(a_1\eta + a_2\eta^2 + a_3\eta^3). \tag{13}$$

Substituting Eq. (13) into the definition of w gives

$$w = \int_0^h u\,\mathrm{d}y = \frac{5}{8}U_i h + \frac{\theta\tau_i h^3}{48\pi\mu r_0} - \frac{\tau_i}{8}\frac{h^2}{\mu} + \left[\frac{\tau_g}{48\mu r_0}\left(2-\frac{\theta}{\pi}\right) - \frac{g h \sin\alpha}{48\mu}\right]h^3, \tag{14a}$$

$$\tau_w = \mu\frac{\partial u}{\partial y}\bigg|_{y=0} = \frac{\mu U_i a_1}{h} = \frac{3\mu U_i}{2h} + \frac{\tau_i}{2}\left(\frac{\theta h}{2\pi r_0} - 1\right) + \frac{h}{4}\left[\tau_g\left(2-\frac{\theta}{\pi}\right)\frac{1}{r_0} - \rho g \sin\alpha\right]. \tag{14b}$$

1.5 Governing equations and initial conditions

$\mathrm{d}x/\mathrm{d}t = U_i$ will give the distance x traveled by the water particle on the interface. Substituting Eqs. (13) and (14) into Eqs. (10) and (11), and differentiating Eq. (9) with respect t, we can complete a closed set of four ordinary differential equations about x, h, τ_i and U_i as follows:

$$\begin{cases} \dfrac{dx}{dt} = U_i, \\ \dfrac{dh}{dt} = b_6 \dfrac{\tau_i}{U_i} + b_7 \dfrac{\tau_i h}{U_i} + b_8 \dfrac{1}{h} + b_9 \dfrac{h}{U_i}, \\ \dfrac{d\tau_i}{dt} = -0.52 c_2 h^{-1.52} w^{0.91} \dfrac{dh}{dt} \qquad (\text{for Ripple flow}), \\ \qquad \left[\text{or } \dfrac{d\tau_i}{dt} = -1.2 c_1 h^{-2.2} w^{0.6} \dfrac{dh}{dt} \qquad (\text{for Pebble flow}) \right], \\ \dfrac{dU_i}{dt} = -\dfrac{8}{5h} \left[\dfrac{dh}{dt} \left(\dfrac{5}{8} U_i + b_1 \tau_i h^2 + b_2 \tau_i h + b_3 h^2 \right) + \dfrac{d\tau_i}{dt} (b_4 h^3 + b_5 h^2) \right]. \end{cases} \tag{15}$$

In the above $b_1, b_2, \cdots, b_9$ are constants independent of h, U_i, τ_i[7].

At time $t = 0$, we get $x_0 = 0$, and from Eq. (1), $h_0 = 0.5 r_0 (1 - \sin\theta/\theta)$; we select $U_{i0} = 7.5$ m/s to coincide with Ref. [5]. The initial shear stress τ_{i0} on the interface is determined by

$$\begin{cases} \tau_{i0} = \tau_g + c_2 h_0^{-0.52} w_0^{0.91}, \\ w_0 = \left(\dfrac{5}{8} U_{i0} h_0 + \dfrac{b_3}{3} h_0^3 \right) + (b_4 h_0^3 + b_5 h_0^2) \tau_{i0}. \end{cases} \tag{16}$$

In our calculations, the bisection method is used to numerically solve Eq. (16) for τ_{i0}.

2 The Varying Thickness Model for Spiral Flow

All the derivations are in parallel to those for axial flow. The only difference lies in the geometry. For spiral flow the water is spread over the whole circumference rather than constricted to the angle θ. To render the results comparable between the axial flow and the spiral flow, we assume that the water layers in the two flows have the same initial cross-section area. Thus the initial thickness h_0 of the axial flow should satisfy the following equation $[0.5 r_0^2 (\theta - \sin\theta)] = 2\pi h_0 r_0$, and then we have $h_0 = (r_0/4\pi)(\theta - \sin\theta)$, which is much smaller than the initial thickness h_0 of the axial flow. For the spiral flow, the volumetric flow rate of water per unit width should be defined as $w = \int_0^h u(1 - y/r_0)\, dy$ and the momentum should be $\int_0^h ul(r_0 - y)\, dy$, where y is the coordinate perpendicular to the wall and starting from the wall. Keeping these differences in mind, one may finally obtain the following governing equations for the spiral flow:

$$\frac{dx}{dt} = U_i, \tag{17a}$$

$$\frac{dh}{dt} = d_1 \frac{\tau_i (3r_0 - 2h)}{(r_0 - h)^2 U_i} + d_2 \frac{h(3r_0 - 2h)}{U_i (r_0 - h)} + d_3 \frac{1}{h(r_0 - h)}, \tag{17b}$$

$$\frac{d\tau_i}{dt} = -0.52 c_2 h^{-1.52} w^{0.91} \frac{dh}{dt} \qquad (U_i' > C\lambda), \tag{17c}$$

$$\left(\text{or } \frac{d\tau_i}{dt} = -1.2 c_1 h^{-2.2} w^{0.6} \frac{dh}{dt} \qquad (U_i' < C\lambda) \right), \tag{17d}$$

$$\frac{dU_i}{dt} = -\frac{1}{(d_6 h - 0.4h^2)}\left\{\frac{dh}{dt}\left[d_4 \frac{\tau_i h^2(3r_0 - 2h)}{(r_0 - h)^2} + d_6 U_i + d_7 \tau_i h(r_0 - h) + d_8 h^2 + d_9 h^3 - 0.8 U_i h\right] + \frac{d\tau_i}{dt}\left[d_4 \frac{h^3}{r_0 - h} + d_5 h^2(3r_0 - 2h)\right]\right\}, \tag{17e}$$

where d_1, d_2, $\cdots$, d_9 are constants independent of h, U_i, τ_i.[7]

The determination of the initial conditions of the spiral flow also can be given just like the axial flow.

3 Results and Discussion

In our examples, the following parameters are taken: ρ = 1 000 kg/m^3, μ = 0.001 Pa·s, r_0 = 39.5 mm, ρ_g = 1.2 kg/m^3, μ_g = 1.8 ×10^{-5} Pa·s, U_g = 20 m/s, the swirl velocity for the spiral flow V_s = 0.25 m/s[5].

The ordinary differential Eqs. (15) and (17) with the initial conditions can be solved numerically through the fourth-order Runge-Kutta method. To discuss the effects of the inclination angle of the pipe and the cross-section area of the residual water on the water purging, we let α = 0, α = 30°, α = 60° and θ = 70°, θ = 50°, θ = 118.115° separately, and get various initial conditions.

The results for the variation of x, U_i and h with t are shown in Fig. 5a and Fig. 5b, and the development of the water velocity profile with time t are shown in Fig. 4a, Fig. 4b and Fig. 6a to Fig. 9b.

From these figures, we can draw the following conclusions:

1) When the inclined angle of the pipe is zero, both kinds of airflow can purge the residual water out, but the spiral flow spends much shorter time than the axial flow to reach the steady state. In the steady state, the velocity of the water film all became positive, so the residual water can flow out of the pipe at last (Please compare Fig. 4a with Fig. 4b).

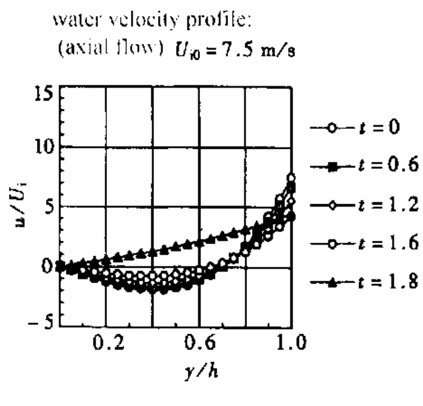

Fig. 4a Axial flow (θ = 70°, α = 0°)

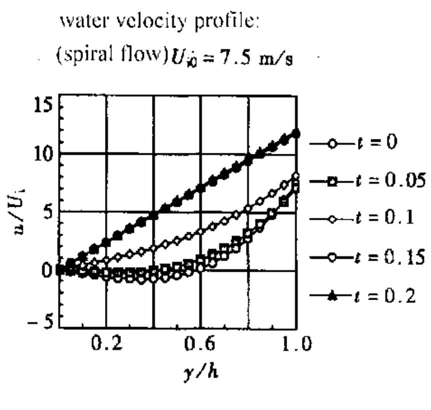

Fig. 4b Spiral flow (θ = 70°, α = 0°)

2) The spiral airflow can purge the residual water in inclined pipe out completely when the amount of water is not too much. The water layer thickness h reduces as t increases (i.e., x

increases), and, at last, the water velocity profile can become all positive and then the water film flow out at this steady velocity profile (Fig. 5b to Fig. 8b). But the axial airflow can remove the water only for cases with small inclined angle (e. g., $\alpha = 30°$) and thin water film (e. g. $\theta = 50°$) (Fig. 7a). In most cases, back flow appears on the water bottom for the axial flow, and the water layer thickness h increases as t increases (i. e., x increases) (Fig. 5a to Fig. 7a). This is coincident with the experimental result of Ref. [5] which showed a back flow after the residual water was driven up for a distance by the axial airflow. It should be noted that, as x increases, the water thickness h in the axial flow may increases to such degree that the back flow of the bottom water may lead to the surface instability. Hence the water surface may be broken into drops and then they flow down, so the residual water can't flow out. In this case, the movement of water can't be described by our continuous model. This prevented from our calculation of the long time behavior for the axial flow cases.

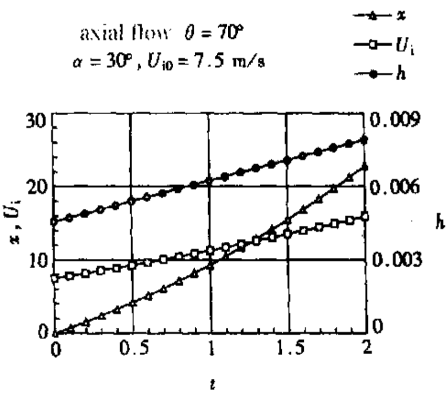

Fig. 5a Axial flow ($\theta = 70°$, $\alpha = 30°$)

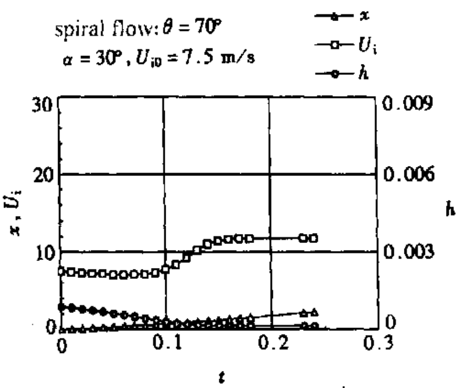

Fig. 5b Spiral flow ($\theta = 70°$, $\alpha = 30°$)

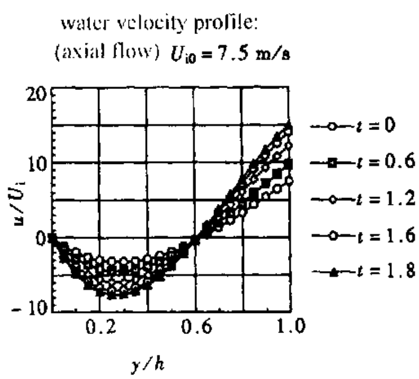

Fig. 6a Axial flow ($\theta = 70°$, $\alpha = 30°$)

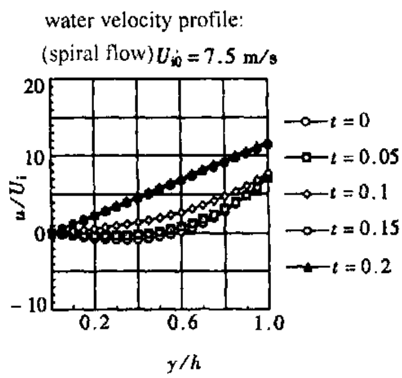

Fig. 6b Spiral flow ($\theta = 70°$, $\alpha = 30°$)

3) When the amount of water is small and the inclined angle is small, both kinds of flow

can remove the residual water (compare Fig. 8a with Fig. 8b), but the time that the axial flow spends to purge the water out completely is 10 times as the spiral flow spends. This suggests that using the spiral flow is much more efficient than using the axial flow.

4) In the case of the residual water with very thick film, if the given spiral flow can't remove the water, larger velocity can often be used to purge the water out. For example, at the initial airflow velocity of U_{i0} = 7.5 m/s a spiral flow could not remove the residual water (θ = 118.115°, Fig. 9a), but at U_{i0} = 12m/s, the water was successfully removed (Fig. 9b). While for the axial flow, our computation reveals that one can't remove the residual water by increasing the velocity of airflow (Figures were not given for the sake of space).

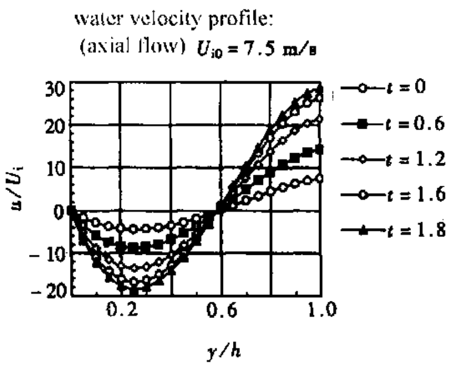

Fig. 7a Axial flow (θ = 70°, α = 60°)

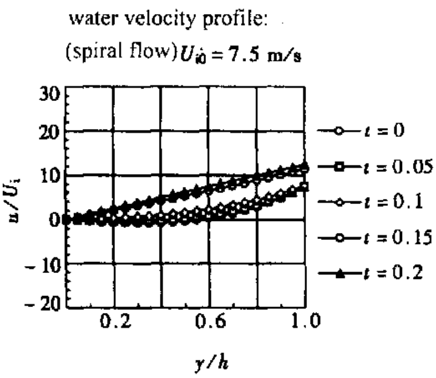

Fig. 7b Spiral flow (θ = 70°, α = 60°)

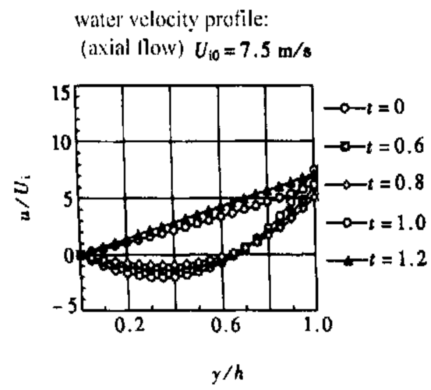

Fig. 8a Axial flow (θ = 50°, α = 30°)

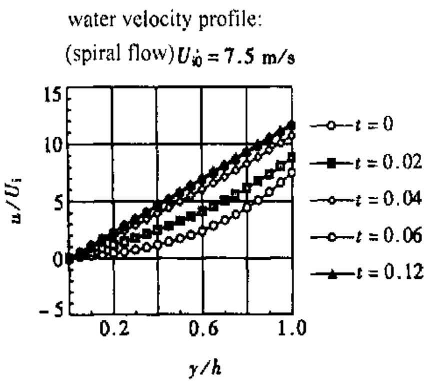

Fig. 8b Spiral flow (θ = 50°, α = 30°)

5) From the figures, we can easily find out that, it is more difficult to remove the residual water when the inclined angle α of the pipe and the thickness of the water gets larger. These findings are the same as the experimental results in Ref. [5].

In summary, our theoretical computation reveal that the spiral flow can purge the residual in the inclined pipe efficiently, while the axial flow can't in most cases, just as predicted in the

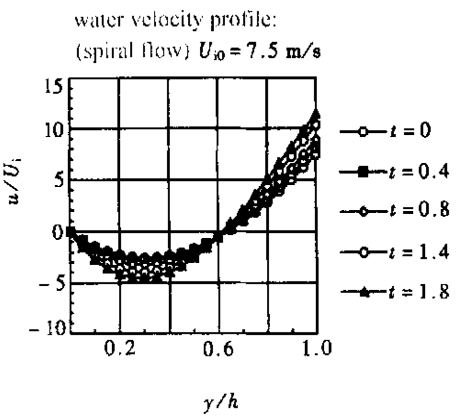

Fig. 9a Spiral flow (θ = 118. 115 °, α = 30 °)

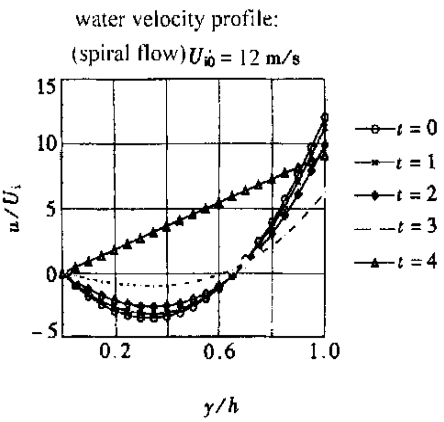

Fig. 9b Spiral flow (θ = 118. 115 °, α = 30 °)

experiment[5]. These results are of significance in guiding the design of water purging from pipeline.

As we stated above, the back flow on the surface of the axial flow may induce great changes in the water surface shape and thus the steady state assumption as we adopted herein will no longer be valid. In order to calculate such complicate cases, unsteady flowing model should be considered in the future research.

References :

[1] Schweinstein A M. Change of flow condition in U-Shaped conduits[J]. Proc Congr Int Assoc Hydraul Res ,1987 ,**22**(3) :280 - 281.

[2] Underwood M P, Kendall C. Vacuum technology for pipeline and system drying[A]. In: The Proc Int Pipeline Technol Exhib Conf[C]. 1984 ,**12**:209 - 226.

[3] Horii K. Using spiral flow for optical cord passing[J]. Mechanical Engineering ,1990 ,**112**(8) :68 - 69.

[4] Horii K, Matsumae Y, Ohsumi K, et al. Novel optical fiber installation by use of spiral airflow [J]. Journal of Fluids Engineerings ,1992 ,**114**(3) :375 - 378.

[5] Horii K, Zhao Y H, Tomita Y, et al. High performance spiral air-flow apparatus for purging residual water in a pipeline [A]. In: D P Telionis Ed. ASME Fluids Engineering Division Summer Meeting[C]. Vancouver: ASME, FEDSM 97-3035 ,1997 ,1 - 6.

[6] Fukano T. Liquid films flowing concurrently with air in horizontal duct[J]. Trans JSME Series B , 1985 ,**51**(462) :494 - 502.

[7] SHEN Fang. Theoretical analysis of using airflow to purge residual water in pipe[D]. Thesis for Bachelor Degree. Beijing: Peking University ,1999 ,1 - 35. (in Chinese)

[8] WU Wang-yi. Fluid Mechanics[M]. Beijing: Peking University Press ,1981 ,**2**:267 - 311. (in Chinese)

[9] ZHOU Guang-jiong , YAN Zong-yi , XU Shi-xiong , et al. Fluid Mechanics[M]. High Education Press ,1993 ,**2**:182 - 302. (in Chinese)